

# MIRAGE: MODEL-AGNOSTIC GRAPH DISTILLATION FOR GRAPH CLASSIFICATION

**Mridul Gupta\***

Yardi School of Artificial Intelligence  
Indian Institute of Technology, Delhi  
Hauz Khas, New Delhi, Delhi, India  
mridul.gupta@scai.iitd.ac.in

**Sahil Manchanda\***

Department of Computer Science  
Indian Institute of Technology, Delhi  
Hauz Khas, New Delhi, Delhi, India  
csz188551@iitd.ac.in

**Hariprasad Kodamana**

Department of Chemical Engineering and Yardi School of Artificial Intelligence (Joint Appointment)  
Indian Institute of Technology, Delhi  
Hauz Khas, New Delhi, Delhi, India  
kodamana@iitd.ac.in

**Sayan Ranu**

Department of Computer Science and Yardi School of Artificial Intelligence (Joint Appointment)  
Indian Institute of Technology, Delhi  
Hauz Khas, New Delhi, Delhi, India  
sayanranu@cse.iitd.ac.in

## ABSTRACT

GNNs, like other deep learning models, are data and computation hungry. There is a pressing need to scale training of GNNs on large datasets to enable their usage on low-resource environments. Graph distillation is an effort in that direction with the aim to construct a smaller synthetic training set from the original training data without significantly compromising model performance. While initial efforts are promising, this work is motivated by two key observations: (1) Existing graph distillation algorithms themselves rely on training with the full dataset, which undermines the very premise of graph distillation. (2) The distillation process is specific to the target GNN architecture and hyper-parameters and thus not robust to changes in the modeling pipeline. We circumvent these limitations by designing a distillation algorithm called MIRAGE for graph classification. MIRAGE is built on the insight that a message-passing GNN decomposes the input graph into a *multi-set of computation trees*. Furthermore, the frequency distribution of computation trees is often skewed in nature, enabling us to condense this data into a concise distilled summary. By compressing the computation data itself, as opposed to emulating gradient flows on the original training set—a prevalent approach to date—MIRAGE transforms into an unsupervised and architecture-agnostic distillation algorithm. Extensive benchmarking on real-world datasets underscores MIRAGE’s superiority, showcasing enhanced generalization accuracy, data compression, and distillation efficiency when compared to state-of-the-art baselines.

## 1 INTRODUCTION AND RELATED WORK

GNNs have shown state-of-the-art performance in various machine learning tasks, including node classification (Hamilton et al., 2017; Veličković et al., 2018), link prediction (Hamilton et al., 2017; Veličković et al., 2018), and graph classification (Ying et al., 2021; Rampášek et al., 2022). Their applications percolate various domains including social networks (Manchanda et al., 2020), drug discovery (Ying et al., 2021; Rampášek et al., 2022) and recommendation engines (Ying et al., 2018). Despite the efficacy of GNNs, like many other deep-learning models, GNNs are data, as well as, computation hungry. This nature of GNNs become particularly more straining when models require frequent retraining to adapt to new training data, as in the case of continual learning (Tang

\*These authors contributed equally to this work

& Matteson, 2021), or when deployed on resource-constrained edge devices like IoT sensors and embedded systems (Miao et al., 2021). Owing to these limitations, the quest for efficient deployment of GNNs has become increasingly imperative.

One important area of study that tackles this problem is the idea of *data distillation* (or condensation) for graphs. In essence, data distillation seeks to compress, or distill, the vital information within a graph dataset while preserving its critical structural and functional properties. The objective in the distillation process is to compress the train data as much as possible without compromising on the predictive accuracy of the GNN when trained on the distilled data. The distilled data therefore significantly alleviates the computational and storage demands, due to which GNNs may be trained more efficiently including on devices with limited resources, like small chips. It is important to note that the distilled dataset need not be a subset of the original data; it may be a fully synthetic dataset.

### 1.1 EXISTING WORKS

Data distillation has proven to be an effective strategy for alleviating the computational demands imposed by deep learning models. For instance, in the case of DC (Zhao et al., 2021), a dataset of  $\approx 60,000$  images was distilled down to just 100 images, resulting in an impressive accuracy of 97.4%, compared to the original accuracy of 99.6%.

Graph distillation has also been explored in prior research (Jin et al., 2022; 2021; Xu et al., 2023). These graph distillation algorithms share a common approach, where the distilled dataset seeks to replicate the same gradient trajectory of the model parameters as seen in the original training set.

In this work, we observe that the process of mimicking gradients necessitates supervision from the original training set, giving rise to significant limitations.

1. **Counter-objective design:** The primary goal in data distillation is to circumvent the need for training on the entire training dataset, given the evident computational and storage constraints. Paradoxically, existing algorithms aim to replicate the gradient trajectory of the original dataset, necessitating training on the full dataset for distillation. Consequently, the fundamental premise of data distillation is compromised.
2. **Dependency on Model and Hyper-Parameters:** The gradients of model weights are contingent on various factors such as the specific GNN architecture and hyper-parameters, including the number of layers, hidden dimensions, dropout rates, and more. As a result, any alteration in the architecture, such as transitioning from a Graph Convolutional Network (GCN) to a Graph Attention Network (GAT), or adjustments to hyper-parameters, necessitates a fresh round of distillation.
3. **Storage Overhead:** Given the dependence of the distillation process on both the GNN architecture and hyper-parameters, a distinct distilled dataset must be maintained for each unique combination of architecture and hyper-parameters. This inevitably amplifies the storage requirements and maintenance overhead.

At this juncture, it is essential to note the difference between graph coarsening (Cai et al., 2021; Ma & Chen, 2019) and graph distillation; seemingly similar terminologies but denoting two distinct approaches. Graph coarsening strives to reduce the dimension of a graph while retaining the essential characteristics of the original input graph, eventually creating a coarser representation of the graph that algorithms can more efficiently process. In contrast, graph distillation attempts to minimize the graph dataset size without compromising the performance of downstream applications.

### 1.2 CONTRIBUTIONS

To address the above outlined limitations of existing algorithms, we design an unsupervised graph distillation algorithm called MIRAGE for graph classification. MIRAGE proposes several innovative strategies imparting significant advantages over existing graph distillation methods.

- **Unsupervised algorithm:** Instead of replicating the gradient trajectory, MIRAGE emulates the input data processed by message-passing GNNs<sup>1</sup>. By shifting the computation task to the pre-learning phase, MIRAGE and the resulting distilled data become independent of hyper-parameters and model architecture (as long as it adheres to a message-passing GNN framework like GAT (Veličković et al., 2018), GCN (Kipf & Welling, 2016), GRAPHSAGE (Hamilton et al., 2017), GIN (Xu et al., 2019), etc.). Moreover, this addresses a critical limitation of existing graph distillation algorithms that necessitate training on the entire dataset.

<sup>1</sup>Hence, the name MIRAGE.

- **Novel GNN-customized algorithm:** MIRAGE exploits the insight that given a graph, an  $\ell$ -layered message-passing GNNs decomposes the graph into a set of computation trees of depth  $\ell$ . Furthermore, the frequency distribution of computation trees often follows a power-law distribution (See. Fig. 1). MIRAGE exploits this pattern by mining the set of frequently co-occurring trees. Subsequently, the GNN is trained by sampling from the co-occurring trees. An additional benefit of this straightforward distillation process is its computational efficiency, as the entire algorithm can be executed on a CPU. This stands in contrast to existing graph distillation algorithms that rely on GPUs, making MIRAGE a more resource and environment friendly alternative.
- **Empirical performance:** We perform extensive benchmarking of MIRAGE against state-of-the-art graph distillation algorithms on six real world-graph datasets and establish that MIRAGE achieves (1) higher prediction accuracy on average, (2) 4 to 5 times higher data compression, and (3) a significant 150-fold acceleration in the distillation process when compared to state-of-the-art graph distillation algorithms.

## 2 PRELIMINARIES AND PROBLEM FORMULATION

In this section, we introduce the preliminary concepts central to our work and formulate the problem of graph distillation for graph classification.

**Definition 1** (Graph). A graph is defined as  $\mathcal{G} = (\mathcal{V}, \mathcal{E}, \mathbf{X})$  over a finite non-empty node set  $\mathcal{V}$  and edge set and  $\mathcal{E} = \{(u, v) \mid u, v \in \mathcal{V}\}$ .  $\mathbf{X} \in \mathbb{R}^{|\mathcal{V}| \times |F|}$  is a node feature matrix where  $F$  is a set of features characterizing each node.

As an example, in case of molecules, nodes and edges would correspond to atoms and bonds, respectively, while features would correspond to properties such as atom type, hybridisation state, etc.

Equivalence between graphs is captured through *graph isomorphism*.

**Definition 2** (Graph Isomorphism). Two graphs  $\mathcal{G}_1$  and  $\mathcal{G}_2$  are considered isomorphic (denoted as  $\mathcal{G}_1 \cong \mathcal{G}_2$ ) if there exists a bijection between their node sets that preserves the edges and node features. Specifically,  $\mathcal{G}_1 \cong \mathcal{G}_2 \iff \exists f : \mathcal{V}_1 \rightarrow \mathcal{V}_2$  such that: (1)  $f$  is a bijection, (2)  $\mathbf{x}_v = \mathbf{x}_{f(v)}$ ,<sup>2</sup> and (3)  $(u, v) \in \mathcal{E}_1$  if and only if  $(f(u), f(v)) \in \mathcal{E}_2$ .

**Graph Classification:** In graph classification, we are given a set of *train* graphs  $\mathcal{D}_{tr} = \{\mathcal{G}_1, \dots, \mathcal{G}_m\}$ , where each graph  $\mathcal{G}_i$  is tagged with a class label  $\mathcal{Y}_i$ . The objective is to train a GNN  $\Phi_{\Theta_{tr}}$  parameterized by  $\Theta_{tr}$  from this train set such that given an unseen set of *validation* graphs  $\mathcal{D}_{val}$  with unknown labels, the label prediction error is minimized. Mathematically, this involves learning the optimal parameter set  $\Theta_{tr}$ , where:

$$\Theta_{tr} = \arg \min_{\Theta} \{\epsilon(\{\Phi_{\Theta}(\mathcal{G}) \mid \forall \mathcal{G} \in \mathcal{D}_{val}\})\} \quad (1)$$

Here,  $\Phi_{\Theta_{tr}}(\mathcal{G})$  denotes the predicted label of  $\mathcal{G}$  by GNN  $\Phi_{\Theta_{tr}}$  and  $\epsilon(\{\Phi_{\Theta}(\mathcal{G}) \mid \forall \mathcal{G} \in \mathcal{D}_{val}\})$  denotes the *error* with parameter set  $\Theta$ . Error may be measured using any of the known metrics such as cross-entropy loss, negative log-likelihood, etc.

Hereon, we implicitly assume  $\Phi$  to be a *message-passing* GNN such as GCN (Kipf & Welling, 2016), GRAPH-SAGE (Hamilton et al., 2017), GAT (Veličković et al., 2018), and GIN (Xu et al., 2019). Furthermore, we assume the validation set to be fixed. Hence, the generalization error of GNN  $\Phi$  when trained on dataset  $\mathcal{D}_{tr}$  is simply denoted using  $\epsilon_{\mathcal{D}_{tr}}$ .

With this background, the problem of graph distillation for graph classification is defined as follows.

**Problem 1** (Graph Distillation). Given a training set and validation set of graphs,  $\mathcal{D}_{tr}$  and  $\mathcal{D}_{val}$ , respectively, generate a dataset  $\mathcal{S}$  from  $\mathcal{D}_{tr}$  with the following dual objectives:

1. **Error:** Minimize the error gap between  $\mathcal{S}$  and  $\mathcal{D}_{tr}$  on the validation set, i.e., minimize  $\{|\epsilon_{\mathcal{S}} - \epsilon_{\mathcal{D}_{tr}}|\}$ .

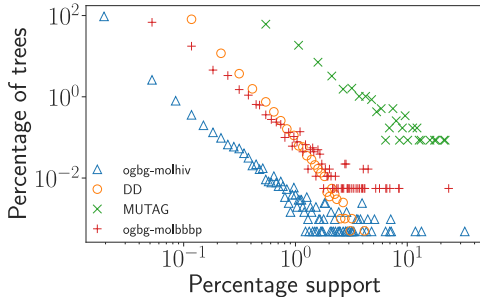


Figure 1: Frequency distribution of computation trees in GNNs. The details of the datasets are in Table 1.

<sup>2</sup>One may relax feature equivalence to having a distance within a certain threshold.

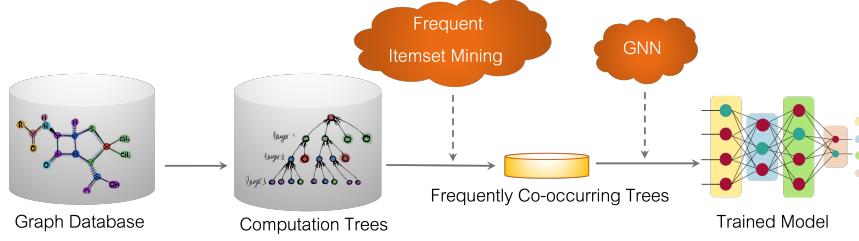


Figure 2: Pipeline of MIRAGE.

2. **Compression:** Minimize the size of  $\mathcal{S}$ . Size will be measured in terms of raw memory consumption, i.e., in bytes.

In addition to the above objectives, we impose two practical constraints on the distillation algorithm. First, it should not rely on the specific GNN architecture, except for the assumption that it belongs to the message-passing family. Second, it should be independent of the model parameters when trained on the original training set. Adhering to these constraints addresses the limitations outlined in § 1.1.

### 3 MIRAGE: PROPOSED METHODOLOGY

MIRAGE exploits the computation framework of message-passing GNNs to craft an effective data compression strategy. Figure. 2 presents the pipeline of MIRAGE. GNNs decompose any graph into a set of computation trees. We mine this set to extract the frequently co-occurring computation trees. As evident from Fig. 1, the frequency distribution of computation trees often follows a power-law. Hence, a compact set of top- $k$  frequently co-occurring trees effectively capture a substantial portion of the distribution mass while retaining a wealth of information content. Subsequently, the GNN is trained only through the frequent tree sets. We next elaborate on each of these intermediate steps and the rationale behind our design choices.

#### 3.1 COMPUTATION FRAMEWORK OF GNNs

GNNs aggregate messages in a layer-by-layer manner. Assuming  $\mathbf{x}_v \in \mathbb{R}^{|F|}$  as the input feature vector for every node  $v \in \mathcal{V}$ , the  $0^{\text{th}}$  layer representation of node  $v$  is simply  $\mathbf{h}_v^0 = \mathbf{x}_v \quad \forall v \in \mathcal{V}$ . Subsequently, in each layer  $\ell$ , GNNs draw messages from its neighbours  $\mathcal{N}_v^1$  and aggregate them as follows:

$$\mathbf{m}_v^\ell(u) = \text{MSG}^\ell(\mathbf{h}_u^{\ell-1}, \mathbf{h}_v^{\ell-1}) \quad \forall u \in \mathcal{N}_v^1 \quad (2)$$

$$\overline{\mathbf{m}}_v^\ell = \text{AGGREGATE}^\ell(\{\{\mathbf{m}_v^\ell(u), \forall u \in \mathcal{N}_v^1\}\}) \quad (3)$$

where  $\text{MSG}^\ell$  and  $\text{AGGREGATE}^\ell$  are either pre-defined functions (Ex: MEANPOOL) or neural networks (GAT (Veličković et al., 2018)).  $\{\{\cdot\}\}$  denotes a multi-set since the same message may be received from multiple nodes. The  $\ell^{\text{th}}$  layer representation of  $v$  is a summary of all the messages drawn.

$$\mathbf{h}_v^\ell = \text{COMBINE}^\ell(\mathbf{h}_v^{\ell-1}, \overline{\mathbf{m}}_v^\ell) \quad (4)$$

where  $\text{COMBINE}^\ell$  is a neural network. Finally, the representation of the graph is computed as:

$$\mathbf{h}_G = \text{COMBINE}(\mathbf{h}_v^L, \forall v \in \mathcal{V}) \quad (5)$$

Here,  $\text{COMBINE}$  could be aggregation functions such as MEANPOOL, SUMPOOL, etc. and  $L$  is total number of layers in the GNN.

#### 3.2 COMPUTATION TREES

We now define the concept of *computation trees* and draw attention to some important properties that sets the base for graph distillation.

**Definition 3** (Computation Tree). *Given graph  $\mathcal{G}$ , node  $v$  and the number of layers  $L$  in a GNN, we construct a computation tree  $\mathcal{T}_v^L$  rooted at  $v$ . Starting from  $v$ , enumerate all paths, including non-simple paths<sup>3</sup>, of  $L$  hops. Next, merge these paths under the following constraints to form  $\mathcal{T}_v^L$ . Two nodes  $v_i$  and  $v'_j$  in paths  $P = \{v_0 = v, v_1, \dots, v_L\}$  and  $P' = \{v'_0 = v, v'_1, \dots, v'_L\}$ , respectively, are merged into a single node in  $\mathcal{T}_v^L$  if either  $i = j = 0$  or  $v_i = v'_j$ ,  $i = j$  and  $\forall k \in [0, i - 1]$ ,  $v_k$  and  $v'_k$  have been merged.*

**Observation 1.** *In an  $L$ -layered GNN, the final representation  $\mathbf{h}_v^L$  of a node  $v$  in graph  $\mathcal{G}$  can be computed from its computation tree  $\mathcal{T}_v^L$ .*

*Proof.* In each layer, a GNN draws messages from its direct neighbors. Over  $L$  layers, a node  $v$  receives messages from nodes reachable within  $L$  hops. All paths of length up to  $L$  from  $v$  are contained within  $\mathcal{T}_v^L$ . Hence, the computation tree is sufficient for computing  $\mathbf{h}_v^L$ .  $\square$

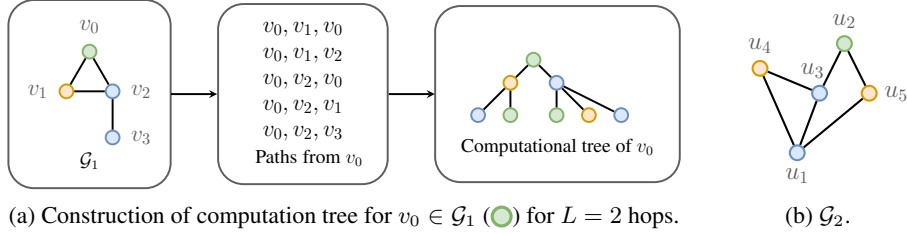


Figure 3: In (a) we show the construction of the computation tree for  $v_0 \in \mathcal{G}_1$ . In (b), we present  $\mathcal{G}_2$ , which has an isomorphic 2-hop computational tree for  $u_2$  despite its neighborhood being non-isomorphic to  $v_0$ . We assume the node feature vectors to be an one-hot encoding of the node colors.

**Observation 2.** If  $\mathcal{T}_v^L \cong \mathcal{T}_u^L$ , then  $\mathbf{h}_v^L = \mathbf{h}_u^L$ .

*Proof.* A message-passing GNN is at most as powerful as *Weisfeiler-Lehman tests (1-WL)* (Xu et al., 2019), which implies that if the  $L$ -hop neighborhoods of nodes  $u$  and  $v$  are indistinguishable by 1-WL, then their representations would be the same. 1-WL cannot distinguish between graphs of identical computation trees (Shervashidze et al., 2011).  $\square$

**Observation 3.** Two nodes with non-isomorphic  $L$ -hop neighborhoods may have isomorphic computation trees.

PROOF. See Figure. 3.  $\square$

**Implications:** Obs. 1 reveals that any graph may be decomposed into a *multiset* of computation trees (not a set since the same tree may appear multiple times) without losing any information. By learning the representations of each computation tree root, we can construct each node representation accurately, and consequently, derive an accurate representation for the entire graph (Recall Eq. 5). Now, suppose the frequency distribution of these computation trees in the multiset is significantly skewed, with a small minority dominating the count. In that case, the graph representation, obtained by aggregating the root representations of only the highly frequent trees, will closely approximate the true graph representation. This phenomenon, illustrated in Figure. 1, is commonly observed. Furthermore, Obs. 3 implies that the set of all computations trees is strictly a subset of the set of all  $L$ -hop subgraphs in the dataset, leading to further skewness in the distribution. Leveraging this pattern, we devise a distillation process that revolves around retaining only those computation trees that *co-occur* frequently. While frequency captures the contribution of a computation tree towards the graph representation, co-occurrence among trees captures frequent graph compositions.

### 3.3 MINING FREQUENTLY CO-OCCURRING COMPUTATION TREES

Let  $\mathbb{T} = \{\mathcal{T}_1, \dots, \mathcal{T}_n\}$  be a set of computation trees. The *frequency* of  $\mathbb{T}$  in the train set  $\mathcal{D} = \{\mathcal{G}_1, \dots, \mathcal{G}_m\}$  is defined as the proportion of graphs that contain all of the computation trees in  $\mathbb{T}$ . Formally,

$$\text{freq}(\mathbb{T}) = \frac{|\{\mathcal{G} \in \mathcal{D} \mid \forall \mathcal{T} \in \mathbb{T}, \exists \mathcal{T}_v^L \in \mathbb{T}_{\mathcal{G}}, \mathcal{T} \cong \mathcal{T}_v^L\}|}{|\mathcal{D}|} \quad (6)$$

Here,  $\mathbb{T}_{\mathcal{G}}$  denotes the set of computation trees in graph  $\mathcal{G}$ .

**Problem 2 (Mining Frequent Co-occurring Trees).** Given a set of  $|\mathcal{D}|$  computation tree multi-sets<sup>4</sup>  $\mathfrak{T} = \{\mathbb{T}_1, \dots, \mathbb{T}_m\}$  corresponding to each graph in the train set  $\mathcal{D} = \{\mathcal{G}_1, \dots, \mathcal{G}_m\}$ , and a threshold  $\theta$ , mine all co-occurring trees with frequency of at least  $\theta$ . Formally, we seek to identify the following distilled answer set.

$$\mathcal{S} = \{\mathcal{X} \subset \mathcal{I} \mid \text{freq}(\mathcal{X}) \geq \theta\} \text{ where } \mathcal{I} = \bigcup_{\forall \mathbb{T}_i \in \mathfrak{T}} \{\mathbb{T}_i\} \quad (7)$$

$\mathcal{I}$  denotes the universe of all unique computation trees, i.e.,  $\forall \mathbb{T}_i, \mathbb{T}_j \in \mathcal{I}, \mathbb{T}_i \not\cong \mathbb{T}_j$ .

We map Problem 2 to the problem of mining frequent itemsets from transaction databases (Han et al., 2004), which we solve using the FPGROWTH algorithm (Han et al., 2004).

### 3.4 MODELING AND INFERENCE

Algorithm. 1 in the appendix outlines the pseudocode of our data distillation and Algorithm. 2 outlines the modeling algorithm. We decompose each graph into their computation trees. We mine the frequently co-occurring trees from each class separately. Instead of training on a batch of graphs,

<sup>3</sup>a non-simple path allows repetition of vertices

<sup>4</sup>non-isomorphic graphs may decompose to the same set of computation trees

we sample a batch of frequent tree sets. Each of these frequent tree sets serves as a surrogate for an entire graph, allowing us to approximate the graph embedding. To achieve this approximation, we utilize the COMBINE function (Eq. 5) on the embeddings of the root node within each tree present in the selected set. The probability of selecting a particular tree set for sampling is directly proportional to its frequency of occurrence.

### 3.5 PROPERTIES AND PARAMETERS

**Parameters:** As opposed to existing graph distillation algorithms (Jin et al., 2022; 2021; Xu et al., 2023), which are dependent on the specific choice of GNN architecture and all hyper-parameters that the GNN relies on, MIRAGE intakes only two parameters: the number of GNN layers  $L$  and the frequency threshold  $\theta$ .  $\theta$ , which lies in  $[0, 1]$ , is a GNN independent parameter. The size of the distilled dataset increases monotonically with decrease in  $\theta$ . Hence,  $\theta$  may be selected based on the desired distillation size.  $L$  is the only model-specific information we require. We note that the number of layers used while training needs to be  $\leq L$ , and need not exactly  $L$ , since  $\mathcal{T}_v^L \supseteq \mathcal{T}_v^{L-1}$ . Hence,  $L$  should be set based on the expected upper limit that may be used. GNNs are typically run with  $L \leq 3$  due to the well-known issue of over-smoothing and over-squashing (Topping et al., 2022).

**Algorithm Characterization:** MIRAGE has several salient characteristics when compared to existing baselines, all arising due to being unsupervised to original training gradients-the predominant approach in graph distillation.

- **Robustness:** The distillation process is independent of training hyper-parameters (except the mild assumption on maximum number of GNN layers) and choice of GNN architecture. Hence, it does not need to be regenerated for changes to any of the above factors.
- **Storage Overhead:** MIRAGE has a smaller storage footprint since a single distilled dataset suffices for all combinations of architecture and hyper-parameters.
- **CPU-bound executions and efficiency:** The distillation pipeline is a function of the training dataset only. Hence, it is computationally efficient requiring only CPU-bound operations.

**Complexity Analysis:** A detailed complexity analysis of MIRAGE is provided in Appendix. A. We also discuss strategies to speed-up tree frequency counting through the usage of *canonical labels*. In summary, the entire process of decomposing the full graph database into computation tree sets incurs  $\mathcal{O}(z \times \delta^L)$  cost, where  $z = \sum_{\mathcal{G} \in \mathcal{D}} |\mathcal{V}|$  and  $\delta$  is the average degree of nodes. Counting frequency of all trees consume  $\mathcal{O}(z \times L \delta^L \log(\delta))$  time. FPGROWTH consumes  $\mathcal{O}(2^{|\mathcal{I}|})$  in the worst case, but it has been shown in the literature that empirical efficiency is dramatically faster due to sparsity in frequent patterns (Han et al., 2004).

## 4 EXPERIMENTS

In this section, we benchmark MIRAGE on 6 real-world datasets and establish that it outperforms the state of the art graph distillation algorithms for graph classification across all three dimensions of prediction accuracy, data compression, and distillation efficiency. Specifically,

- **Accuracy:** MIRAGE is the most robust distillation algorithm and consistently ranks among the top-2 performers across all dataset-GNN combinations.
- **Compression:** MIRAGE achieves the highest compression on average, which is  $\approx 4$  and  $\approx 5$  times smaller than the state of the art algorithms of DOSCOND and KIDD respectively.
- **Efficiency:** MIRAGE is  $\approx 150$  and  $\approx 500$  times faster than DOSCOND and KIDD on average.

its efficacy and efficiency for graph distillation. All experiments have been executed 5 times. We report the mean and standard deviations. The codebase of MIRAGE is shared anonymously <https://anonymous.4open.science/r/Mirage>. For details on the hardware and software platform used, please refer to App. B.1 in the appendix.

### 4.1 DATASETS

To evaluate MIRAGE, we use datasets from *Open Graph Benchmark* (OGB) (Hu et al., 2020) and *TU Datasets* (DD, IMDB-B and NCI1) (Morris et al., 2020) spanning a variety of domains. The

Table 1: Dataset statistics

Dataset	#Classes	#Graphs	Avg. Nodes	Avg. Edges	Domain
ogbg-molbace	2	1513	34.1	36.9	Molecules
NCI1	2	4110	29.9	32.3	Molecules
ogbg-molbbbp	2	2039	24.1	26.0	Molecules
ogbg-molhiv	2	41,127	25.5	54.9	Molecules
DD	2	1178	284.3	715.7	Proteins
IMDB-B	2	1000	19.39	193.25	Movie

Table 2: AUC-ROC of benchmarked algorithms across datasets and GNN architectures. The best and the second best AUC-ROC in each dataset is highlighted in dark and light green colors respectively. We do not report the results of GAT in IMDB-B since this dataset does not contain in any node features. GAT struggles to learn attention in this scenario and achieves an AUC-ROC of  $\approx 0.5$  across the full datasets and their distilled versions for all baselines.

Dataset	Model	RANDOM (mean)	RANDOM (sum)	HERDING	KIDD	DOSCOND	MIRAGE	Full Dataset
ogbg-molbace	GAT	65.43 $\pm$ 3.57	73.75 $\pm$ 2.30	58.39 $\pm$ 7.04	66.16 $\pm$ 4.62	68.30 $\pm$ 1.01	72.71 $\pm$ 3.41	77.20 $\pm$ 2.20
	GCN	62.96 $\pm$ 3.25	76.03 $\pm$ 0.60	52.46 $\pm$ 6.47	63.92 $\pm$ 13.1	67.34 $\pm$ 1.84	75.90 $\pm$ 3.11	77.31 $\pm$ 1.60
	GIN	57.18 $\pm$ 10.4	74.95 $\pm$ 2.28	65.24 $\pm$ 6.17	77.09 $\pm$ 0.57	63.41 $\pm$ 0.66	76.21 $\pm$ 0.67	78.53 $\pm$ 3.70
NC11	GAT	50.46 $\pm$ 2.65	64.01 $\pm$ 6.87	66.77 $\pm$ 1.11	60.62 $\pm$ 1.47	58.10 $\pm$ 1.52	68.10 $\pm$ 0.20	83.50 $\pm$ 0.71
	GCN	51.36 $\pm$ 0.36	60.72 $\pm$ 8.06	66.86 $\pm$ 0.73	64.85 $\pm$ 2.32	57.90 $\pm$ 0.75	68.20 $\pm$ 0.04	87.03 $\pm$ 0.57
	GIN	51.60 $\pm$ 5.85	61.15 $\pm$ 7.30	67.12 $\pm$ 1.90	60.83 $\pm$ 2.26	59.80 $\pm$ 2.30	67.91 $\pm$ 0.31	85.60 $\pm$ 2.19
ogbg-molbbbp	GAT	57.16 $\pm$ 2.20	60.40 $\pm$ 1.84	59.15 $\pm$ 4.13	62.88 $\pm$ 3.31	61.12 $\pm$ 2.51	63.05 $\pm$ 1.10	64.70 $\pm$ 2.10
	GCN	60.18 $\pm$ 2.66	58.76 $\pm$ 3.51	55.93 $\pm$ 1.09	58.77 $\pm$ 1.83	59.19 $\pm$ 0.95	61.30 $\pm$ 0.52	64.43 $\pm$ 2.21
	GIN	60.06 $\pm$ 3.85	60.21 $\pm$ 3.14	54.88 $\pm$ 2.84	64.21 $\pm$ 0.99	61.10 $\pm$ 2.10	61.21 $\pm$ 0.77	64.95 $\pm$ 2.24
ogbg-molhiv	GAT	53.35 $\pm$ 4.78	64.61 $\pm$ 8.43	61.82 $\pm$ 1.75	69.79 $\pm$ 0.64	72.33 $\pm$ 0.85	71.78 $\pm$ 2.18	66.34 $\pm$ 1.38
	GCN	48.21 $\pm$ 5.95	67.20 $\pm$ 6.16	59.36 $\pm$ 2.79	69.56 $\pm$ 2.74	73.16 $\pm$ 0.69	70.13 $\pm$ 1.44	64.78 $\pm$ 2.33
	GIN	53.07 $\pm$ 7.07	69.94 $\pm$ 1.42	69.66 $\pm$ 2.64	63.02 $\pm$ 4.48	72.72 $\pm$ 0.80	71.55 $\pm$ 1.70	65.13 $\pm$ 3.07
DD	GAT	50.87 $\pm$ 1.10	67.31 $\pm$ 12.0	71.20 $\pm$ 2.14	73.14 $\pm$ 4.32	63.45 $\pm$ 2.47	72.96 $\pm$ 2.78	76.36 $\pm$ 0.09
	GCN	53.58 $\pm$ 2.38	58.02 $\pm$ 8.57	65.26 $\pm$ 5.63	71.04 $\pm$ 6.04	68.39 $\pm$ 9.64	76.14 $\pm$ 1.59	75.37 $\pm$ 1.23
	GIN	57.34 $\pm$ 1.60	67.50 $\pm$ 9.66	73.23 $\pm$ 3.62	64.55 $\pm$ 3.50	60.23 $\pm$ 1.76	75.19 $\pm$ 0.85	74.74 $\pm$ 0.58
IMDB-B	GCN	52.06 $\pm$ 4.90	50.38 $\pm$ 0.31	60.69 $\pm$ 3.43	58.29 $\pm$ 0.61	55.56 $\pm$ 2.83	59.17 $\pm$ 0.07	60.84 $\pm$ 2.50
	GIN	51.31 $\pm$ 4.10	51.12 $\pm$ 2.76	60.48 $\pm$ 3.28	57.45 $\pm$ 0.16	60.02 $\pm$ 2.49	62.18 $\pm$ 0.17	66.73 $\pm$ 1.53

chosen datasets represent sufficient diversity in graph sizes ( $\approx 24$  nodes to  $\approx 284$  nodes) and density ( $\approx 1$  to  $\approx 10$ ).

## 4.2 EXPERIMENTAL SETUP

**Baselines.** Among neural baselines, we consider the state of the art graph distillation algorithms for graph classification, which are (1) DOSCOND (Jin et al., 2022) and (2) KIDD (Xu et al., 2023). We do not consider GCOND (Jin et al., 2021) since DOSCOND have been shown to consistently outperform GCOND. KIDD supports graph distillation only GIN. We also include (3) HERDING (Welling, 2009) maps graphs into embeddings using the target GNN architecture. Subsequently, it selects the graphs that are closest to the cluster centers in the distilled set. Finally, we consider the (4) RANDOM baseline, wherein we randomly select graphs over iterations from each class in the dataset till the combined size exceeds the size of the distilled dataset produced by MIRAGE. Comparing with RANDOM highlights the impact of the information content within frequent computation trees as opposed to a roughly equal proportion of trees selected uniformly at random from the dataset.

**Evaluation Protocol.** We benchmark MIRAGE and considered baselines across three different GNN architectures, namely GCN (Kipf & Welling, 2016), GAT (Veličković et al., 2018) and GIN (Xu et al., 2019). It is worth noting that this is the first graph distillation study to span three GNN architectures when compared DOSCOND or KIDD, that evaluate only on a specific GNN of choice.

The evaluation framework proceeds under the following pipeline. First each GNN architecture is trained on the full dataset to collect the gold-standard data. Next, we distill the dataset using each of the chosen baselines. The same GNN model is now trained on the distilled dataset, whose performance we report. For model-agnostic algorithms, which are MIRAGE and RANDOM, the same distilled dataset is used for all GNN architectures. In contrast, the distillation dataset is architecture-specific for DOSCOND and HERDING. KIDD only supports GIN. Hence, for other GNN architectures, we use the distilled dataset for GIN, but train using the target GNN.

**Train-validation-test Splits.** The OGB datasets come with the train-validation-test splits, which are also used in DOSCOND and KIDD. For TU Datasets, we randomly split the graphs into 80%/10%/10% for training-validation-test. We stop the training of a model if it does not improve the validation loss for more than 15 epochs.

**Metrics.** To measure prediction accuracy, we use AUC-ROC. The size of all distillation datasets are reported in the unit of *bytes*. In addition, we also measure the graph distillation time.

**Parameter settings.** Hyper-parameters used to train MIRAGE, the baselines, and the GNN models are discussed in Appendix. B.2.

Table 3: Size of distilled dataset, in terms of *bytes*, produced by benchmarked algorithms across datasets and GNN architectures. The best compression is highlighted in dark green color. The results for IMDB-B for GAT represented as - are skipped since GAT achieves  $\approx 0.5$  AUC-ROC on IMDB-B.

Method $\rightarrow$ Dataset $\downarrow$	HERDING			KIDD	DOSCOND			MIRAGE	Full Dataset
	GAT	GCN	GIN		GAT	GCN	GIN		
ogbg-molbace	25,771	26,007	26,129	2,592	23,176	23,176	23,176	1,612	1,610,356
NC11	5,662	5,680	5,683	26,822	70,168	70,760	73,128	318	1,046,828
ogbg-molbbbp	10,497	10,514	10,466	3,618	13,632	14,280	20,832	6,108	740,236
ogbg-molhiv	21,096	21,096	21,140	7,672	4,808	5,280	4,400	3,288	41,478,694
DD	89,882	89,869	90,086	408,980	210,168	210,184	209,816	448	7,414,218
IMDB-B	-	1,238	1,252	980	-	1184	2484	280	635,856

### 4.3 PERFORMANCE IN GRAPH DISTILLATION

**Prediction Accuracy.** In Table 2, we report the mean and standard deviation of the testset AUC-ROC of all baselines on the distilled dataset as well as the AUC-ROC when trained on the full dataset. Several important insights emerge from Table 2.

Firstly, it is noteworthy that MIRAGE consistently ranks as either the top performer or the second-best across all combinations of datasets and architectures. Particularly striking is the fact that MIRAGE achieves the best performance in 8 out of the 17 dataset-architecture combinations, which stands as the highest number of top rankings among all considered baselines. This demonstrates that the unsupervised nature of MIRAGE does not come at the expense of prediction accuracy.

Secondly, we observe instances where the distilled dataset outperforms the full dataset, an outcome that might initially seem counter-intuitive. This phenomenon has been reported in the literature before (Xu et al., 2023). While pinpointing the exact cause behind this behavior is challenging, we hypothesize that the distillation process may tend to remove outliers from the training set, subsequently leading to improved accuracy. Additionally, given that distillation prioritizes the selection of graph components that are more informative to the task, it is likely to retain the most critical patterns, resulting in enhanced model generalizability.

Finally, we note that the performance of RANDOM (sum), which involves random graph selection and the COMBINE function (Eq. 5) being SUMPOOL, is surprisingly strong, and at times surpassing the performance of all baselines. Interestingly, in the literature, DOSCOND and KIDD have reported results only with RANDOM (mean), which is substantially weaker. We investigated this phenomenon and noticed that in datasets where RANDOM (sum) performs well, the label distribution of nodes and the number of nodes across the classes are noticeably different. SUMPOOL is better at preserving these magnitude differences in node and label counts compared to MEANPOOL, which averages them out.

**Compression.** We next investigate the size of the distilled dataset. MIRAGE is independent of the underlying GNN architecture, ensuring that its size remains consistent regardless of the specific architecture employed. On the other hand, KIDD, as previously indicated in § 4.2, conducts distillation with the assumption that GIN serves as the underlying GNN architecture. In the case of DOSCOND and HERDING, these methods support various GNN architectures; however, the size of the distilled datasets is architecture-specific for each. It is important to note that we exclude RANDOM from this analysis as, per our discussion in § 4.2, we select graphs until the dataset’s size exceeds that of MIRAGE. Consequently, by design, its size closely aligns with that of MIRAGE.

In Table 3, we present the compression results. MIRAGE stands out by achieving the highest compression in 5 out of 6 datasets. In the single dataset where it does not hold the smallest size, MIRAGE still ranks as the second smallest, showcasing its consistent compression performance. On average, MIRAGE achieves a compression rate that is  $\approx 4$  times higher compared to DOSCOND and 5 times greater than KIDD. This notable advantage of MIRAGE over the baseline methods underscores the effectiveness of exploiting data distribution over replicating gradients, at least within the context of graph databases where recurring patterns are prevalent.

**Distillation Time.** We now focus on the efficiency of the distillation process. Fig. 4 presents this information. We observe that MIRAGE is more than  $\approx 500$  times faster on average than KIDD and  $\approx 150$  times faster than DOSCOND. This impressive computational-efficiency is achieved despite MIRAGE utilizing only a CPU for its computations, whereas DOSCOND and KIDD are reliant on GPUs. This trend is a direct consequence of MIRAGE not being dependent on training on the full data. KIDD is slower than DOSCOND since, while both seek to replicate the gradient trajectory



of model weights, KIDD solves this optimization problem exactly, whereas DOSCOND is an approximation. Overall, MIRAGE is not only faster, but also presents a more environment-friendly and energy-efficient approach to graph distillation.

#### 4.4 IMPACT OF PARAMETERS

**Training efficiency.** We now investigate the reduction in training loss over the course of multiple epochs. The outcomes for the datasets ogbg-molbace, ogbg-mohiv, DD, and IMDB-B are displayed in Fig. 5. We selected these four datasets due to their representation of the smallest and largest graph dataset, the dataset with the largest graphs, and the densest graphs, respectively. Across all these datasets, the loss in the distilled dataset remains close to the loss in the full dataset. More interestingly, in three out of four datasets (DD and IMDB-B), the loss begins at a substantially lower value in the distilled dataset and approaches the minima quicker than in the full dataset. This trend provides evidence of MIRAGE’s ability to achieve a dual objective. By identifying frequently co-occurring computation trees, we simultaneously preserve the most informative patterns within the dataset while effectively removing noise.

**Impact of Frequency Threshold.** Fig. 6 presents the impact of frequency threshold on distillation efficiency. The distillation size and time is expected to increase monotonically with the decrease in the threshold since more tree sets qualify as frequent. We observe that even at low thresholds of 1%, MIRAGE remains efficient and significantly faster than baseline algorithms (reported in Table E).

## 5 CONCLUSIONS, LIMITATIONS AND FUTURE WORKS

Training Graph Neural Networks (GNNs) on large-scale graph datasets can be computationally intensive and resource-demanding. To address this challenge, one potential solution is to distill the extensive graph dataset into a more compact synthetic dataset while maintaining competitive predictive accuracy. While the concept of graph distillation has gained attention in recent years, existing methods typically rely on model-related information, such as gradients or embeddings. In this research endeavor, we introduce a novel framework named MIRAGE, which employs a frequent pattern mining-based approach. MIRAGE leverages the inherent design of message-passing frameworks, which decompose graphs into computation trees. It capitalizes on the observation that the distribution of these computation trees often exhibits a highly skewed nature. This unique feature enables us to compress the computational data itself without requiring access to specific model details or hyper-parameters, aside from a reasonable assumption regarding the maximum number of GNN layers. Our extensive experimentation across six real-world datasets, in comparison to state-of-the-art algorithms, demonstrates MIRAGE’s superiority across three critical metrics: predictive accuracy, a distillation efficiency that is 150 times higher, and data compression rates that are 4 times higher. Moreover, it’s noteworthy that MIRAGE solely relies on CPU-bound operations, offering a more environmentally sustainable alternative to existing algorithms.

**Limitations and Future Works:** MIRAGE, as well as, existing graph distillation algorithms currently lack the ability to generalize effectively to unseen tasks. Moreover, their applicability to other types of graphs, such as temporal networks, remains unexplored. Additionally, there is a need to assess how these existing algorithms perform on contemporary architectures like graph transformers (e.g., (Ying et al., 2021; Rampásek et al., 2022)) or equivariant GNNs (e.g., (Satorras et al., 2022)). Our future work will be dedicated to exploring these avenues of research.

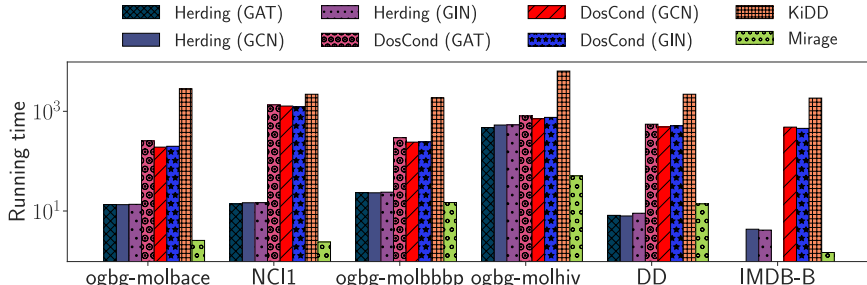


Figure 4: Distillation times for the different methods. Full numbers and standard deviations are in Table E in Appendix.

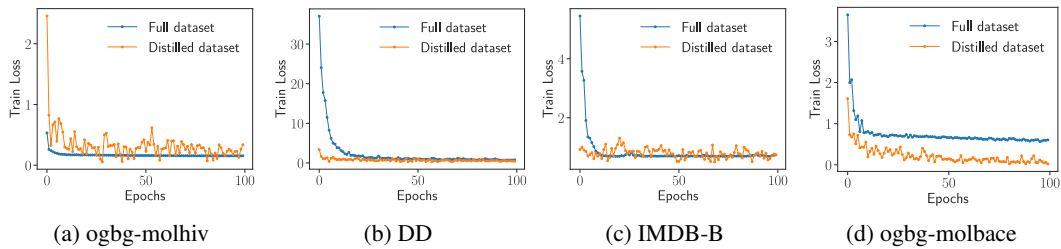
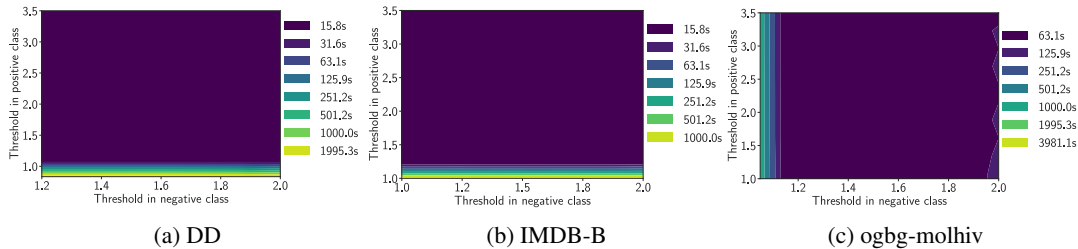


Figure 5: Variation of training loss against the number of epochs in GCN.

Figure 6: Impact of frequency threshold (both positive and negative classes) on the distillation time. Here, the thresholds on the positive and negative classes are varied in the  $y$  and  $x$  axis respectively, and the time is presented as a contour.

## REFERENCES

- Chen Cai, Dingkan Wang, and Yusu Wang. Graph coarsening with neural networks. In *International Conference on Learning Representations*, 2021. URL <https://openreview.net/forum?id=uxpzitPEooJ>. (Cited on p. 2  $\leftrightarrow$ )
- Douglas M. Campbell and David Radford. Tree isomorphism algorithms: Speed vs. clarity. *Mathematics Magazine*, 64(4):252–261, 1991. ISSN 0025570X, 19300980. URL <http://www.jstor.org/stable/2690833>. (Cited on p. 13  $\leftrightarrow$ )
- Yun Chi, Yirong Yang, and Richard R. Muntz. Canonical forms for labelled trees and their applications in frequent subtree mining. *Knowledge and Information Systems*, 8(2):203–234, Aug 2005. ISSN 0219-3116. doi: 10.1007/s10115-004-0180-7. URL <https://doi.org/10.1007/s10115-004-0180-7>. (Cited on p. 13  $\leftrightarrow$ )
- William L. Hamilton, Rex Ying, and Jure Leskovec. Inductive representation learning on large graphs. In *Proceedings of the 31st International Conference on Neural Information Processing Systems, NIPS’17*, pp. 1025–1035, Red Hook, NY, USA, 2017. Curran Associates Inc. ISBN 9781510860964. (Cited on pp. 1, 2, and 3  $\leftrightarrow$ )
- Jiawei Han, Jian Pei, Yiwen Yin, and Runying Mao. Mining frequent patterns without candidate generation: A frequent-pattern tree approach. *Data Mining and Knowledge Discovery*, 8(1):53–87, January 2004. (Cited on pp. 5, 6, and 13  $\leftrightarrow$ )
- Weihua Hu, Matthias Fey, Marinka Zitnik, Yuxiao Dong, Hongyu Ren, Bowen Liu, Michele Catasta, and Jure Leskovec. Open graph benchmark: Datasets for machine learning on graphs. *Advances in neural information processing systems*, 33:22118–22133, 2020. (Cited on p. 6  $\leftrightarrow$ )
- Wei Jin, Lingxiao Zhao, Shichang Zhang, Yozen Liu, Jiliang Tang, and Neil Shah. Graph condensation for graph neural networks. In *International Conference on Learning Representations*, 2021. (Cited on pp. 2, 6, and 7  $\leftrightarrow$ )
- Wei Jin, Xianfeng Tang, Haoming Jiang, Zheng Li, Danqing Zhang, Jiliang Tang, and Bing Yin. Condensing graphs via one-step gradient matching. In *Proceedings of the 28th ACM SIGKDD Conference on Knowledge Discovery and Data Mining*, pp. 720–730, 2022. (Cited on pp. 2, 6, and 7  $\leftrightarrow$ )
- Thomas N Kipf and Max Welling. Semi-supervised classification with graph convolutional networks. *arXiv preprint arXiv:1609.02907*, 2016. (Cited on pp. 2, 3, and 7  $\leftrightarrow$ )

- Tengfei Ma and Jie Chen. Unsupervised learning of graph hierarchical abstractions with differentiable coarsening and optimal transport. In *AAAI Conference on Artificial Intelligence*, 2019. URL <https://api.semanticscholar.org/CorpusID:209460875>. (Cited on p. **2** ↔)
- Sahil Manchanda, Akash Mittal, Anuj Dhawan, Sourav Medya, Sayan Ranu, and Ambuj Singh. Gcomb: Learning budget-constrained combinatorial algorithms over billion-sized graphs. *Advances in Neural Information Processing Systems*, 33:20000–20011, 2020. (Cited on p. **1** ↔)
- Weiwei Miao, Zeng Zeng, Mingxuan Zhang, Siping Quan, Zhen Zhang, Shihao Li, Li Zhang, and Qi Sun. Workload prediction in edge computing based on graph neural network. In *2021 IEEE Intl Conf on Parallel & Distributed Processing with Applications, Big Data & Cloud Computing, Sustainable Computing & Communications, Social Computing & Networking (ISPA/BDCLOUD/SocialCom/SustainCom)*, pp. 1663–1666, 2021. doi: 10.1109/ISPA-BDCLOUD-SocialCom-SustainCom52081.2021.00223. (Cited on p. **2** ↔)
- Christopher Morris, Nils M Kriege, Franka Bause, Kristian Kersting, Petra Mutzel, and Marion Neumann. Tudataset: A collection of benchmark datasets for learning with graphs. *arXiv preprint arXiv:2007.08663*, 2020. (Cited on p. **6** ↔)
- Ladislav Rampásek, Mikhail Galkin, Vijay Prakash Dwivedi, Anh Tuan Luu, Guy Wolf, and Dominique Beaini. Recipe for a General, Powerful, Scalable Graph Transformer. *Advances in Neural Information Processing Systems*, 35, 2022. (Cited on pp. **1 and 9** ↔)
- Victor Garcia Satorras, Emiel Hoogeboom, and Max Welling. E(n) equivariant graph neural networks. In *ICML*, 2022. (Cited on p. **9** ↔)
- Nino Shervashidze, Pascal Schweitzer, Erik Jan van Leeuwen, Kurt Mehlhorn, and Karsten M. Borgwardt. Weisfeiler-lehman graph kernels. *J. Mach. Learn. Res.*, 12(null):2539–2561, nov 2011. ISSN 1532-4435. (Cited on p. **5** ↔)
- Binh Tang and David S. Matteson. Graph-based continual learning. In *ICLR*, 2021. (Cited on p. **1** ↔)
- Jake Topping, Francesco Di Giovanni, Benjamin Paul Chamberlain, Xiaowen Dong, and Michael M. Bronstein. Understanding over-squashing and bottlenecks on graphs via curvature. In *ICLR*, 2022. (Cited on p. **6** ↔)
- Gabriel Valiente. *Tree Isomorphism*, pp. 151–251. Springer Berlin Heidelberg, Berlin, Heidelberg, 2002. ISBN 978-3-662-04921-1. doi: 10.1007/978-3-662-04921-1.4. URL <https://doi.org/10.1007/978-3-662-04921-1.4>. (Cited on p. **13** ↔)
- Petar Veličković, Guillem Cucurull, Arantxa Casanova, Adriana Romero, Pietro Liò, and Yoshua Bengio. Graph attention networks. In *International Conference on Learning Representations*, 2018. URL <https://openreview.net/forum?id=rJXPikCZ>. (Cited on pp. **1, 2, 3, 4, and 7** ↔)
- Max Welling. Herding dynamical weights to learn. In *Proceedings of the 26th Annual International Conference on Machine Learning*, pp. 1121–1128, 2009. (Cited on p. **7** ↔)
- Keyulu Xu, Weihua Hu, Jure Leskovec, and Stefanie Jegelka. How powerful are graph neural networks? In *International Conference on Learning Representations*, 2019. URL <https://openreview.net/forum?id=ryGs6iA5Km>. (Cited on pp. **2, 3, 5, and 7** ↔)
- Zhe Xu, Yuzhong Chen, Menghai Pan, Huiyuan Chen, Mahashweta Das, Hao Yang, and Hanghang Tong. Kernel ridge regression-based graph dataset distillation. In *Proceedings of the 29th ACM SIGKDD Conference on Knowledge Discovery and Data Mining, KDD '23*, pp. 2850–2861, New York, NY, USA, 2023. Association for Computing Machinery. ISBN 9798400701030. doi: 10.1145/3580305.3599398. URL <https://doi.org/10.1145/3580305.3599398>. (Cited on pp. **2, 6, 7, and 8** ↔)
- Chengxuan Ying, Tianle Cai, Shengjie Luo, Shuxin Zheng, Guolin Ke, Di He, Yanming Shen, and Tie-Yan Liu. Do transformers really perform badly for graph representation? In A. Beygelzimer, Y. Dauphin, P. Liang, and J. Wortman Vaughan (eds.), *Advances in Neural Information Processing Systems*, 2021. URL <https://openreview.net/forum?id=OeWooOxFwDa>. (Cited on pp. **1 and 9** ↔)

Rex Ying, Ruining He, Kaifeng Chen, Pong Eksombatchai, William L. Hamilton, and Jure Leskovec. Graph convolutional neural networks for web-scale recommender systems. In *KDD*, pp. 974–983, 2018. (Cited on p. [1](#) ↔)

Bo Zhao, Konda Reddy Mopuri, and Hakan Bilen. Dataset condensation with gradient matching. In *ICLR*, 2021. (Cited on p. [2](#) ↔)

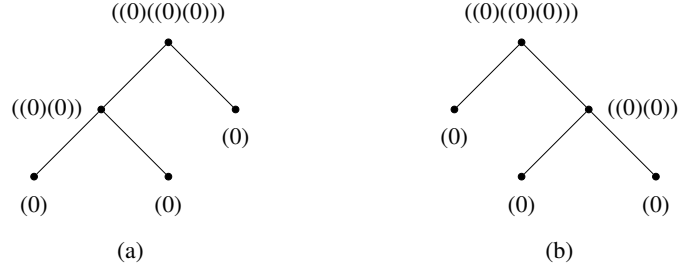


Figure G: (a) and (b) show Knuth Tuples based canonical labels for two isomorphic trees. The process starts at the leaves and goes up to the root. Whenever a node encapsulates its children’s labels, it sorts them in increasing order of length. This can be adapted for the cases when nodes have labels and when the edges have labels by making appropriate changes to the tuples.

## APPENDIX

### A COMPLEXITY ANALYSIS

**Computation tree decomposition:** Each graph  $\mathcal{G} = (\mathcal{V}, \mathcal{E}, \mathbf{X})$ , decomposes into  $|\mathcal{V}|$  computation trees. Assuming an average node degree of  $\delta$ , enumerating a computation tree consumes  $\mathcal{O}(\delta^L)$  time. Hence, the entire process of decomposing the full graph database into computation tree sets incurs  $\mathcal{O}(z \times \delta^L)$  computation cost, where  $z = \sum_{\mathcal{G} \in \mathcal{D}} |\mathcal{V}|$ .

**Frequency counting:** Computing the frequency of a computation tree requires us to perform tree isomorphism test. Although no polynomial time algorithm exists for graph isomorphism, in rooted trees, it can be performed in linear time to the number of nodes in the tree (Valiente, 2002), which in our context is  $\mathcal{O}(\delta^L)$ . Thus, frequency counting of all trees requires  $\mathcal{O}(\delta^L \times z^2)$  time. In MIRAGE, we optimize frequency counting further using *canonical labeling* (Campbell & Radford, 1991).

**Definition 4** (Canonical label). *A canonical label of a graph  $\mathcal{G}$  involves defining a unique representation or labeling of a graph in a way that is invariant under isomorphism. Specifically, if  $\mathcal{L}$  is the function that maps a graph to its canonical label, then*

$$\mathcal{G}_1 \cong \mathcal{G}_2 \iff \mathcal{L}(\mathcal{G}_1) = \mathcal{L}(\mathcal{G}_2)$$

There are several algorithms available described in (Campbell & Radford, 1991) and (Chi et al., 2005) that map rooted-trees to canonical labels. We use (Campbell & Radford, 1991) in our implementation, which is explained in Fig. G.

Canonical label construction for a rooted tree consumes  $\mathcal{O}(m \log(m))$  time if the tree contains  $m$  nodes. In our case,  $m = \mathcal{O}(\delta^L)$  as discussed earlier. Thus, the complexity is  $\mathcal{O}(\delta^L \log(\delta^L)) = \mathcal{O}(L \delta^L \log(\delta))$  time. Once trees have been constructed, frequency counting involves hashing each of the canonical labels, which takes linear time to the number of graphs. Hence, the complexity reduces to  $\mathcal{O}(z \times L \delta^L \log(\delta))$  when compared to the all pairs tree isomorphism approach of  $\mathcal{O}(\delta^L \times z^2)$  ( $L \log(\delta) \ll z$ ).

**Frequent itemset mining:** Finally, in the frequent itemset mining step, the complexity in the worst case is  $\mathcal{O}(2^{|\mathcal{I}|})$ . In reality, however, the running times are dramatically smaller due to majority of items (trees in our context) being infrequent (and hence itemsets as well) (Han et al., 2004).

### B EMPIRICAL SETUP

#### B.1 HARDWARE AND SOFTWARE PLATFORM

All experiments are performed on an Intel Xeon Gold 6248 processor with 96 cores and 1 NVIDIA A100 GPU with 40GB memory, and 377 GB RAM with Ubuntu 18.04. In all experiments, we have trained using the Adam optimizer with a learning rate of 0.0001 and choose the model based on the best validation loss.

**Algorithm 1** MIRAGE: Proposed graph distillation algorithm

---

**Input** Train set  $\mathcal{D}$ , number of layers  $L$  in GNN, frequency threshold  $\theta$ .  
**Output** Distilled dataset  $\mathcal{S}$  and parameters  $\Theta$  of the GNN when trained on  $\mathcal{S}$

- 1:  $\mathcal{S} \leftarrow \emptyset$
- 2: **for each** Class  $c$  in dataset **do**
- 3:      $\mathfrak{T}_c \leftarrow \emptyset$
- 4:     **for each**  $\mathcal{G} = (\mathcal{V}, \mathcal{E}, \mathbf{X}) \in \mathcal{D}$  such that  $\mathcal{Y}_{\mathcal{G}} = c$  **do**
- 5:          $\mathbb{T} \leftarrow \emptyset$
- 6:         **for each**  $v \in \mathcal{V}$  **do**
- 7:              $\mathbb{T} \leftarrow \mathbb{T} \cup \{\mathcal{T}_v^L = \text{compute-tree}(\mathcal{G}, v, L) \mid \forall v \in \mathcal{V}\}$
- 8:          $\mathfrak{T}_c \leftarrow \mathfrak{T}_c \cup \mathbb{T}$
- 9:      $\mathcal{S} \leftarrow \mathcal{S} \cup \text{FPGROWTH}(\mathfrak{T}_c, \theta)$
- 10: **Return**  $\mathcal{S}$

---

**Algorithm 2** Training a GNN using data distilled using MIRAGE

---

**Input** Distilled dataset  $\mathcal{S}$   
**Output** Parameters  $\Theta$  of the GNN when trained on  $\mathcal{S}$

- 1: Randomly initialize  $\Theta$
- 2: **while** Model loss has not converged **do**
- 3:      $\mathfrak{B} \leftarrow$  a batch of tree sets sampled in proportion to their frequencies from  $\mathcal{S}$
- 4:     **for each**  $\mathbb{T} \in \mathfrak{B}$  **do**
- 5:          $\mathbf{h}_{\mathbb{T}} \leftarrow \text{COMBINE}(\mathbf{h}_v^L, \forall \mathcal{T}_v^L \in \mathbb{T})$
- 6:     Update  $\Theta$  using backpropagation based on loss over  $\{\mathbf{h}_{\mathbb{T}} \mid \forall \mathbb{T} \in \mathfrak{B}\}$
- 7: **Return**  $\Theta$

---

## B.2 PARAMETERS

Table Da presents the parameters used to train MIRAGE. Note that the same distillation parameters are used for all benchmarked GNN architectures and hence showcasing its robustness to different flavors of modeling pipelines.

For neural baselines KIDD and DOSCOND, we use the same parameters recommended in their respective papers on datasets that are also used in their studies. Otherwise, the optimal parameters are chosen using grid search.

For the model hyper-parameters, we perform grid search to optimize performance on the whole dataset. The same parameters are used to train and infer on the distilled dataset. The hyper-parameters used are shown in Table Db.

## C DISTILLATION GENERALIZATION OF DOSCOND

While message-passing GNNs come in various architectural forms, one may argue that the embeddings generated, when the data and the loss are same, are correlated. Hence, even in the case of GNN-dependent distillation algorithms, such as DOSCOND, it stands to reason that the same distil-

Table D: Parameters used for MIRAGE.

(a) Distillation parameters.  $\theta_0$  and  $\theta_1$  represent the frequency thresholds in class 0 () and 1 respectively.

Dataset	$\theta_0$	$\theta_1$	#hops ( $L$ )
NC11	27%	35%	2
ogbg-molbbbp	5%	7%	2
ogbg-molbace	13%	10%	3
ogbg-molhiv	5%	8%	3
DD	2%	2%	1
IMDB-B	20%	20%	1

(b) Model parameters

Model	Layers	Hidden Dimension	Dropout	Reduce Type
GCN	{2, 3}	{64, 128}	[0, 0.6]	{sum, mean}
GAT	{2, 3}	{64, 128}	[0, 0.6]	{sum, mean}
GIN	{2, 3}	{64, 128}	[0, 0.6]	{sum, mean}

Table E: Graph distillation time (in seconds) consumed by various algorithms.

Method → Dataset ↓	HERDING			DOSCOND			KIDD	MIRAGE
	GAT	GCN	GIN	GAT	GCN	GIN		
ogbg-molbace	13.47 ± 0.52	13.41 ± 0.57	13.62 ± 0.72	255.62 ± 7.52	191.22 ± 5.62	198.89 ± 6.21	2839.40	2.57 ± 0.12
NCI1	13.86 ± 0.29	14.64 ± 0.48	14.70 ± 0.43	1348.21 ± 11.2	1275.82 ± 13.2	1237.98 ± 82.5	2200.04	2.39 ± 0.16
ogbg-molbbbp	23.35 ± 1.59	23.18 ± 1.33	23.86 ± 1.32	295.02 ± 3.34	240.91 ± 7.58	244.44 ± 5.33	1855.81	14.78 ± 0.09
ogbg-molhiv	473.44 ± 23.8	530.89 ± 27.8	535.08 ± 32.74	808.11 ± 42.3	708.33 ± 7.54	755.48 ± 54.9	6421.98	50.86 ± 0.32
DD	8.18 ± 0.51	7.95 ± 0.57	9.02 ± 0.56	551.39 ± 8.36	485.81 ± 3.79	511.14 ± 4.13	2201.09	13.93 ± 0.16
IMDB-B	-	4.31 ± 0.52	4.14 ± 0.63	-	482.01 ± 4.21	455.02 ± 3.98	1841.80	1.47 ± 0.01

Table F: **Cross-arch performance:** The performance of DOSCOND when graph distillation is performed using gradients of a particular GNN, while the model is trained on another GNN.

$\frac{\text{train+test} \rightarrow}{\text{condensed using} \downarrow}$	GAT	GCN	GIN
GAT	<b>61.12 ± 2.51</b>	<b>59.86 ± 1.50</b>	59.36 ± 1.26
GCN	59.33 ± 3.37	59.19 ± 0.95	57.02 ± 3.09
GIN	58.20 ± 1.91	56.42 ± 1.68	<b>61.10 ± 2.10</b>

(a) ogbg-molbbbp

$\frac{\text{train+test} \rightarrow}{\text{condensed using} \downarrow}$	GAT	GCN	GIN
GAT	<b>68.30 ± 1.01</b>	67.01 ± 4.21	62.90 ± 4.84
GCN	63.70 ± 2.98	<b>67.34 ± 1.84</b>	58.91 ± 4.85
GIN	65.7 ± 3.81	66.47 ± 3.83	<b>63.41 ± 0.66</b>

(b) ogbg-molbace

lation data could generalize well to other GNNs. In Table F, we investigate this hypotheses. Across the six evaluated combinations, except for the case of GCN in OGBG-MOLBBBP, we consistently observe that the highest performance is achieved when the distillation GNN matches the training GNN. This behavior is unsurprising since although GNNs share the initial task of breaking down input graphs into individual components of message-passing trees, subsequent computations diverge. For instance, GIN employs SUMPOOL, which is density-dependent and retains magnitude information. Conversely, GCN, owing to their normalization based on node degrees, does not preserve magnitude information as effectively. GAT, on the other hand, utilizes attention mechanisms, resulting in varying message weights learned as a function of the loss. In summary, Table F provides additional evidence supporting the necessity for GNN-independent distillation algorithms.